Design and Simulation of a Control System For the Bucket Wheel Excavator

DAN DANDEA, MARIN NAN
Department of Mechanical, Industrial Engineering and Transports
University of Petrosani
20 University Street, 332006, Petrosani
ROMANIA
dandea_dan@yahoo.com, nan.marins@gmail.com, www.upet.ro

Abstract: - In this paper is presented the design of an automatic control system for bucket wheel excavators digging at a constant rate. Obtaining a material flow with the smallest variation during the excavation leads to advantages related to intensive use and capacity of all machines that are part of the technological chain. Simulation and implementation of the mathematical model are performed using MatLab Simulink software.

Key-Words: - Bucket wheel excavator, mathematic model, control system, constant flow, simulation

1 Introduction

Cutting and pivoting speed control to achieve an approximately constant flow of material excavated, leads to maintain the power operated equipment positioned downstream to a value close to the nominal, is an area in which currently are made extensive research in the world. Obtaining an material flow with the smallest variation during the excavation leads to advantages related to intensive use and capacity of all machines that are part of the technological chain

2 The mathematical model and the simulation diagram

The simulation diagram of the excavation flow control system of the BWE designed and proposed to be used is shown in figure 1.

The simulation process to be automated is based on the calculation of momentary capacity relationship of excavation:[8]

$$Q_{ma} = 3600 \cdot \frac{h_0}{2 \cdot \pi} \cdot \left(1 - \cos\left(\alpha_0\right)\right) \cdot \frac{v_p \cdot v_t}{\frac{z}{n_c}} \qquad (1)$$

where: h_0 is maximum cutting thickness [m]; α_0 is the cut angle [degrees]; v_p is the pivoting speed; v_t is cutting speed; z is the number of bucket discharges; n_c is the number of buckets on the wheel;

In the simulation process is taken into account that the pivoting speed in equation (1) can be calculated with the formula:

$$v_p = \cos(\theta) \cdot v_p(\theta) \qquad (2)$$

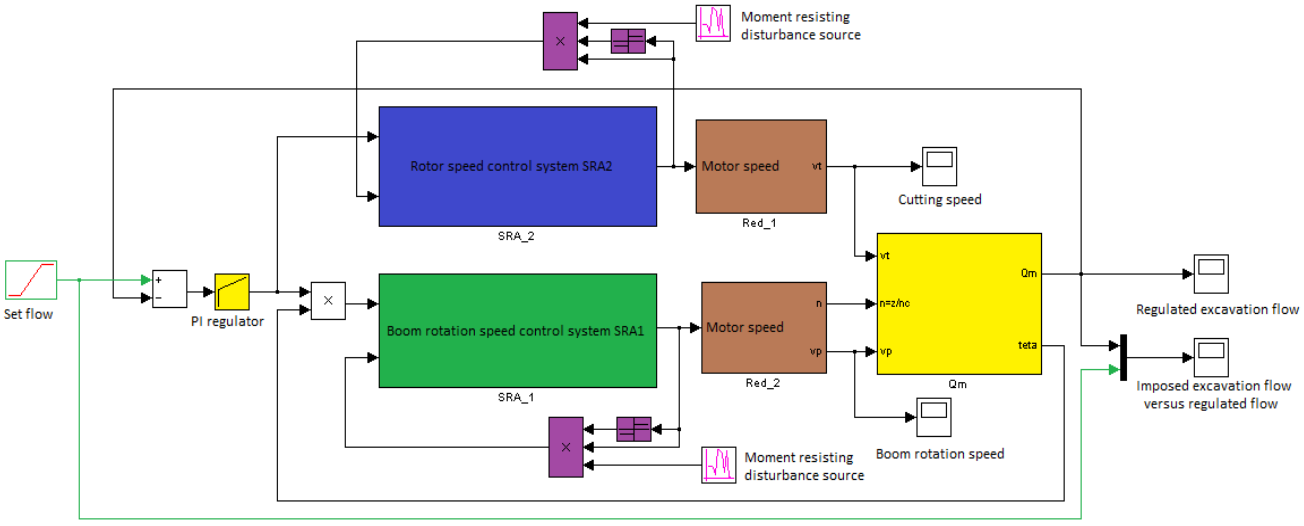

Fig. 1 Simulation diagram of the automated adjustment system of the coal flow used on the bucket wheel excavators.

ISBN: 978-1-61804-171-5

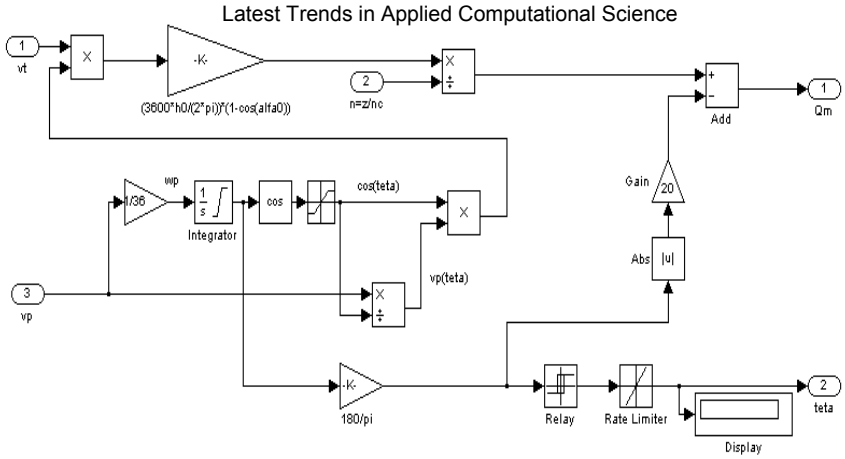

Fig. 2 MatLab Simulink model of the excavation process

The simulation diagram of the excavation process is shown in figure 2. In the simulation it was assumed that the output size of the excavation process is influenced by a disturbing factor of excavation, denoted by Q_{mb}. This disturbance is directly proportional to the absolute total momentary pivot angle.

$$Q_{mb} = k \cdot |\theta| \tag{3}$$

Given the above, momentary excavation capacity can be expressed by the relationship:

$$Q_m = Q_{ma} - Q_{mb} \tag{4}$$

In the simulation algorithm, the total pivoting angle was limited to a range of values between θ_{min} and θ_{max} through a nonlinear saturation type element. To reverse the direction of rotation of the motor that controls the pivoting arm, in the simulation was taken into account the θ_{min}, θ_{max} imposed maximum pivotation angles. In this sense, was used an real bipozitional relay that has the output value 1 when the θ angle exceeds θ_{max} respectively value -1 when the θ angle falls below θ_{min}. Output value marked with "θ" is multiplied by the output value of the flow control system and the result is the required rotation speed imposed to the control system of the induction motor that drives the pivoting arm of the excavator.

2.1 The presentation of a vector oriented control system of induction motors.

The control systems SRA1 and SRA2 are rotor flux vector oriented control systems of the speed of the induction machines. Both control systems are identical with the except that the motors power whose speed is adjusted is different.

The simulation diagram of rotor flux vector oriented control systems of the speed of the induction machine is presented in figure 3.

To achieve the simulation presented above were developed two mathematical models.

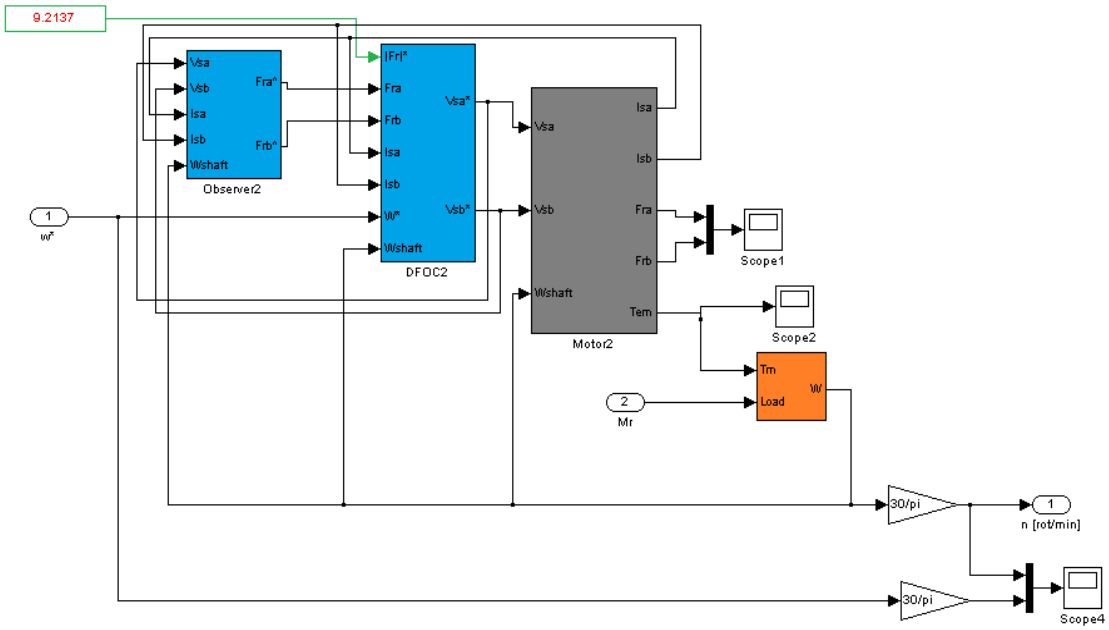

Fig. 3 Simulation diagram of control system SRA2

2.1.1 The mathematical model stator current - rotor flux.

The mathematical model of the induction motor is made as a canonical system status, varying over time, which is as follows:[3]

$$\begin{cases} \frac{d}{dt}x(t) = A(t)\cdot x(t) + B\cdot u(t) \\ y(t) = C\cdot x(t) \end{cases} \quad (5)$$

State vector, x(t), is composed of stator current and rotor flux written in the orthogonal reference $d\lambda - q\lambda$, arbitrarily chosen:

$$x(t) = \left[i_{ds\lambda}(t) \quad i_{qs\lambda}(t) \quad \psi_{dr\lambda}(t) \quad \psi_{qr\lambda}(t) \right]^T \quad (6)$$

Input vector u(t), is composed by the statoric voltages written in the same orthogonal reference:

$$u(t) = \left[u_{ds\lambda}(t) \quad u_{qs\lambda}(t) \right]^T \quad (7)$$

as for the output vector is identical to the state vector:

$$y(t) = x(t) \quad (8)$$

The matrixes that define the canonic system (5), corresponding to stator current - rotor flux model are:

$$A(t) = \begin{bmatrix} a_{11} & 0 & a_{13} & a_{14}\cdot z_p\cdot\omega_r(t) \\ 0 & a_{11} & -a_{14}\cdot z_p\cdot\omega_r(t) & a_{13} \\ a_{31} & 0 & a_{33} & -z_p\cdot\omega_r(t) \\ 0 & a_{31} & z_p\cdot\omega_r(t) & a_{33} \end{bmatrix}$$

$$B = \begin{bmatrix} b_{11} & 0 & 0 & 0 \\ 0 & b_{11} & 0 & 0 \end{bmatrix}^T ; \quad C = I_4 \quad (9)$$

where:

$$a_{11} = -\left(\frac{1}{T_s\cdot\sigma} + \frac{1-\sigma}{T_r\cdot\sigma} \right) ; \; a_{13} = \frac{L_m}{L_s\cdot L_r\cdot T_r\cdot\sigma} ;$$

$$a_{14} = \frac{L_m}{L_s\cdot L_r\cdot\sigma} ; \; a_{31} = \frac{L_m}{T_r} ; \; a_{33} = -\frac{1}{T_r} ;$$

$$b_{11} = \frac{1}{L_s\cdot\sigma} ; \; T_s = \frac{L_s}{R_s} ; \; T_r = \frac{L_r}{R_r} ; \; \sigma = 1 - \frac{L_m^2}{L_s\cdot L_r} .$$

where I_4 is the matrix unit.

The movement equation of the induction motor corresponding to the model to stator current - rotor flux model is:

$$\frac{d}{dt}\omega_r(t) = H_{m1}\cdot\begin{pmatrix} \psi_{dr\lambda}(t)\cdot i_{qs\lambda}(t) - \\ -\psi_{qr\lambda}(t)\cdot i_{ds\lambda}(t) \end{pmatrix} - \quad (10)$$
$$-H_{m2}\cdot\omega_r(t) - H_{m3}\cdot M_r(t)$$

where:

$$H_{m1} = \frac{3}{2}\cdot\frac{z_p}{J}\cdot\frac{L_m}{L_r} ; \; H_{m2} = \frac{F}{J} ; H_{m3} = \frac{1}{J} ;$$

J is the rotor inertia moment;

F is the frictions coefficient;

ω_r is the rotor mechanical angular speed;

The simulation diagram of the engine is based on state equations (5), model called voltage model. Simulation is done using the Simulink-Matlab S_Function block.

Simulation Diagram, internal structure and program developed in Matlab is given to the S_Function block shown in figure 4.

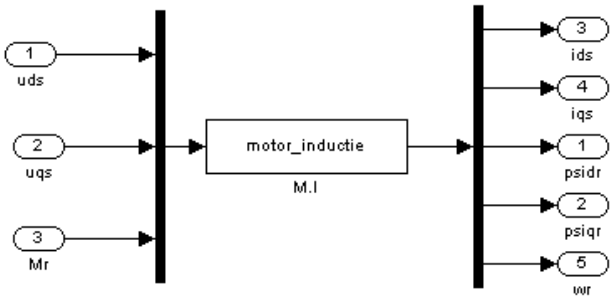

Fig. 4 Induction motor simulation diagram

2.1.2 The mathematical model of the rotoric flux observer.

The Luenberger observer is defined by these equations [9]:

$$\begin{cases} \frac{d}{dt}\hat{x}(t) = A(t)\cdot\hat{x}(t) + B\cdot u(t) + L(t)\cdot\left(y(t) - \hat{y}(t)\right) \\ \hat{y}(t) = C\cdot\hat{x}(t) \end{cases} \quad (11)$$

where:

$$A(t) = \begin{bmatrix} a_{11} & 0 & a_{13} & a_{14}\cdot z_p\cdot\omega_r(t) \\ 0 & a_{11} & -a_{14}\cdot z_p\cdot\omega_r(t) & a_{13} \\ a_{31} & 0 & a_{33} & -z_p\cdot\omega_r(t) \\ 0 & a_{31} & z_p\cdot\omega_r(t) & a_{33} \end{bmatrix}$$

$$B=\begin{bmatrix} b_{11} & 0 & 0 & 0 \\ 0 & b_{11} & 0 & 0 \end{bmatrix}^T;\ C=\begin{bmatrix} 1 & 0 & 0 & 0 \\ 0 & 1 & 0 & 0 \end{bmatrix}$$

and coefficients that define these matrixes are the ones corresponding stator current - rotor flux.

The input, output and state vectors that define the Luenberger estimator are:

$$u(t)=\begin{bmatrix} u_{ds}(t) & u_{qs}(t) \end{bmatrix}^T$$

$$x(t)=\begin{bmatrix} i_{ds}(t) & i_{qs}(t) & \psi_{dr}(t) & \psi_{qr}(t) \end{bmatrix}^T$$

$$y(t)=\begin{bmatrix} i_{ds}(t) & i_{qs}(t) \end{bmatrix}^T$$

and the estimated output, state magnitude vectors are:

$$\hat{x}(t)=\begin{bmatrix} \hat{i}_{ds}(t) & \hat{i}_{qs}(t) & \hat{\psi}_{dr}(t) & \hat{\psi}_{qr}(t) \end{bmatrix}^T$$

$$\hat{y}(t)=\begin{bmatrix} \hat{i}_{ds}(t) & \hat{i}_{qs}(t) \end{bmatrix}^T$$

Matrix L, from the Luenberger estimator is determined in the continuous case, so that the real part of the estimator poles to be strictly negative. In the case of designing the L matrix of the estimator, is taken into account that the values of matrix A, have the real part strictly negative. The most utilized solutions for on-line calculation of Luenberger matrix are:

- the equations that assure the proportionality between the machines poles and the observers poles;
- the method of self-values rotation;
- the method of self-values movement;

Next tis presented the structure of the Luenberger L matrix:

$$L(t)=\begin{bmatrix} l_{11} & -l_{12} \\ l_{12} & l_{11} \\ l_{21} & -l_{22} \\ l_{22} & l_{21} \end{bmatrix} \quad (14)$$

where:

$$\begin{cases} l_{11}=(1-k)\cdot\left(a_{11}^*+a_{33}^*\right) \\ l_{12}=z_p\cdot\omega_r\cdot(1-k) \\ l_{22}=-\gamma\cdot l_{12} \\ l_{21}=\left(a_{31}^*+\gamma\cdot a_{11}^*\right)\cdot\left(1-k^2\right)-\gamma\cdot l_{11} \end{cases} \quad (15)$$

Based on the above entries in the block called Observer in figure 3, Luenberger estimator simulation is performed using specific blocks of Matlab - Simulink.

Within the speed induction motor control system - SRA2 that drives the pivoting arm, the induction machine used has the following characteristics:

$$P_N=160[\mathrm{KW}];\ U_N=400[\mathrm{V}];\ n_N=1487\left[\frac{\mathrm{rot}}{\mathrm{min}}\right];$$

$$f_N=50[\mathrm{Hz}];\ z_p=2;\ R_s=0.01379[\Omega];$$

$$R_r=0.007728[\Omega];\ L_s=0.007842[\mathrm{H}];$$

$$L_r=0.007842[\mathrm{H}];\ L_m=0.00769[\mathrm{H}];$$

$$J=2.9\left[\mathrm{Kg}\cdot\mathrm{m}^2\right];\ F=0.05658\left[\frac{\mathrm{N}\cdot\mathrm{m}\cdot\mathrm{s}}{\mathrm{rad}}\right].$$

Within the speed induction motor control system - SRA1 that drives the bucket wheel, the induction machine used has the following characteristics:

$$P_N=630[\mathrm{KW}];\ U_N=6[\mathrm{kV}];\ n_N=1487\left[\frac{\mathrm{rot}}{\mathrm{min}}\right];$$

$$f_N=50[\mathrm{Hz}];\ z_p=2;\ R_s=0.0453[\Omega];$$

$$R_r=0.0222[\Omega];\ L_s=0.0067[\mathrm{H}];$$

$$L_r=0.0066[\mathrm{H}];\ L_m=0.0065[\mathrm{H}];$$

$$J=10.8\left[\mathrm{Kg}\cdot\mathrm{m}^2\right];\ F=0.004878\left[\frac{\mathrm{N}\cdot\mathrm{m}\cdot\mathrm{s}}{\mathrm{rad}}\right].$$

3 Simulation and result interpretation

Following the simulation the resulting diagrams provide information about the dynamics of the control system process for the excavation.

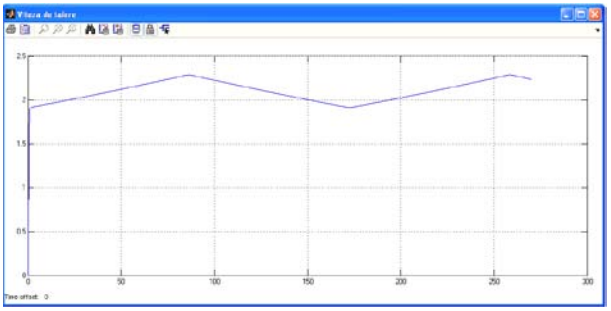

Fig. 5 Cutting wheel speed diagram/time

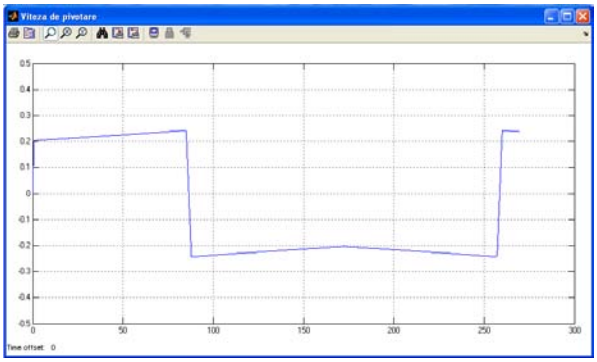

Fig. 6 Time variation of pivoting speed

ISBN: 978-1-61804-171-5

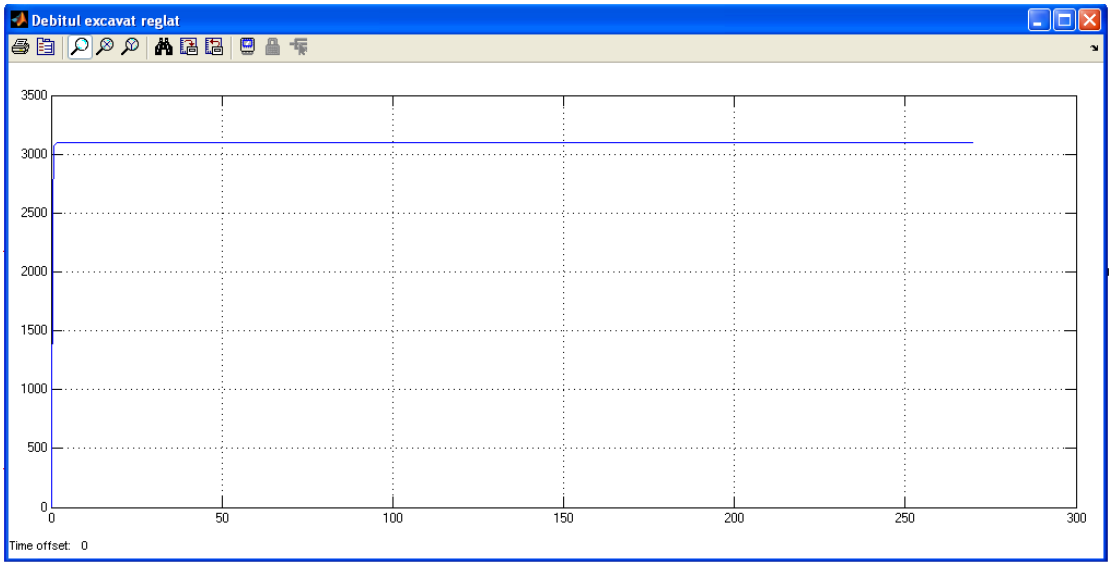

Fig. 7 Time variation of cutting flow (imposed)

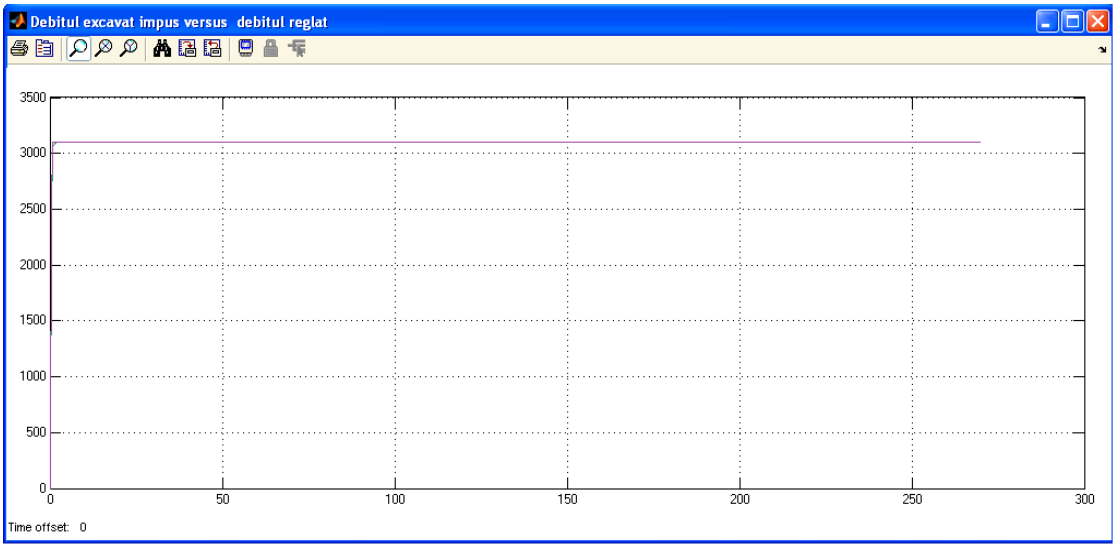

Fig. 8 Time variation of imposed flow (purple) and controlled flow (green)

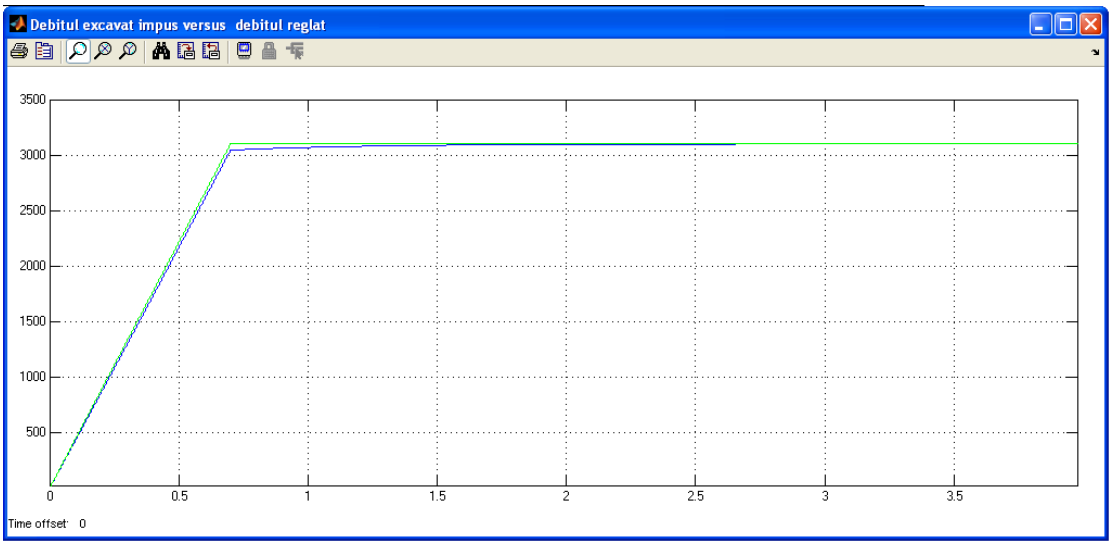

Fig. 9 Time variation of imposed flow (green) and controlled flow (blue) during transient time

ISBN: 978-1-61804-171-5

5 Conclusion

From the diagram analysis it can be seen that the imposed flow is equal to excavation flow with the mention that in the transient time there is a certain difference, this time period corresponds to the speeding up the process to nominal motors speed. These observations confirm the accuracy and the correctness of the designed model.

References:

[1] Al-Bahaddly I., Energy Saving with Variable Speed Drives in Industry Application, *Proc. WSEAS Int. Conf. on Circuits, Systems, Signal and Telecommunication*, 2007.

[2] Barbu C., Some principles design of a local integrated sustainable renewable energetic system, *Mining Journal*, Vol. 17, No.2, Petrosani, 2011.

[3] Kubota H., Matsuse K., Nakano T., New Adaptive Flux observer of Induction Motor for Wide Speed range Motor Drives, *in Proc. Int. Conf. IEEE IECON*, pp. 921-926, 1990.

[4] Schauder C., Adaptive Speed Identification for Vector Control of Induction Motors without Rotational Transducers, *IEEE Trans. Ind. Applicat.*, Vol.28, no.5, pp. 1054-1061, 1992.

[5] Stoicuta O., Campian H., Pana T., (2005) Transfer Function Determination for Vector-Controlled Induction Motor Drives, *ELECTROMOTION*, Lausanne, Switzerland, pp. 316-321.

[6] Stoicuta O., Nan M.S., Dimirache G., Buda N., Dandea D., Research regarding the design of an new transport pipe flow control system, *Proc. WSEAS Int. Conf. Application of Electical Engineering*, 2010.

[7] Stoicuta O., Nan M.S., Dimirache G., Buda N., Dandea D., Research Regarding the Use of New Systems to Control Fluid Flow in Pipelines, *WSEAS TRANSACTIONS on FLUID MECHANICS*, Issue 3, Volume 5, pp 144-154, 2010.

[8] Nan M.S., Ridzi T.I., Dandea D.L., *Transport systems theory*, Universitats Publishing House, 2011.

[9] Popov M., *Hyperstability of Control Systems* (1973) Springer Verlag, New York.

[10] Vamvu P.M., Pop E., Design of a dedicated video controller with specific VLSI Technology, *Universitaria Simpro 2008, sectiunea system control applied informatics and computer engineering*, Petrosani, Romania, ISSN 1842-4449, 2008.

[11] Pop E., *Control engineering in mining industry (Automatizari in industria miniera)*, Editura Didactica si Pedagogica, Bucuresti, Romania, 1983.